



for negative Wigner function is unnecessarily too high to conclusively prove that light is already beyond any mixture of Gaussian states [25]. In addition, homodyne tomography is too demanding for many experiments due to required mode matching to the local oscillator.

In this paper, we propose a direct detection of quantum non-Gaussian light from a single atom in the cavity, which employs single-photon avalanche photo-diodes (SPADs) in Hanbury-Brown and Twiss configuration instead of performing the homodyne tomography. Importantly, this method allows us to detect quantum non-Gaussian light from a single atom in the leaky cavity limit when the negative Wigner function is not observable. It enables investigation of quantum non-Gaussian features produced by discrete levels in a broad class of current atomic and solid-state experiments. Such experiments will further open a general theoretical and experimental investigation of such light sources and stimulate further steps in this part of photonics and quantum technology.

## 2 Quantum non-Gaussianity

The quantum non-Gaussianity identifies light that is prepared beyond states evolving from the vacuum according to the Hamiltonian at most quadratic in the annihilation and creation operators. The unitary operators that the quantum non-Gaussianity overcomes involve the displacement operator  $D(\alpha) = \exp(\alpha a^\dagger - \alpha^* a)$  and the squeezing operator  $S(\xi) = \exp\left[\xi (a^\dagger)^2 - \xi^* a^2\right]$ , which generates an arbitrary Gaussian state by their acting on the vacuum state. Thus, light represented by the density matrix  $\rho$  manifests the quantum non-Gaussianity when

$$\rho \neq \int d^2\xi d^2\alpha P(\xi, \alpha) S(\xi) D(\alpha) |0\rangle \langle 0| D^\dagger(\alpha) S^\dagger(\xi), \quad (1)$$

where  $P(\xi, \alpha)$  stands for a density probability function of the parameters  $\xi$  and  $\alpha$ . Recognition of the quantum non-Gaussianity under realistic conditions of current experiments can employ the Hanbury-Brown and Twiss detection scheme [26], which is depicted in Fig. 1 (a). It consists of a beam-splitter (BS) and two single-photon avalanche photo-diodes SPAD<sub>1</sub> and SPAD<sub>2</sub>. A criterion [27, 28] of the quantum non-Gaussianity

compares their response with a threshold defined in terms of success probability  $P_s$  and error probability  $P_e$  corresponding to a probability of a click on SPAD<sub>1</sub> and a simultaneous click on both SPAD<sub>1</sub> and SPAD<sub>2</sub>, respectively. The quantum non-Gaussianity manifests itself when a state exhibits the probabilities  $P_s$  and  $P_e$  that surpass the threshold

$$P_s = 1 - 4e^{-\frac{1-t^2}{2t(1+3t)}} \sqrt{\frac{t}{3t^2 + 10t + 3}} \quad (2)$$

$$P_e = 1 - 8e^{-\frac{1-t^2}{2t(1+3t)}} \sqrt{\frac{t}{3t^2 + 10t + 3}} + e^{-\frac{(t-1)(t+3)}{2t(1+3t)}} \frac{\sqrt{t}}{1+t},$$

which is expressed by a parameter  $t \in (0, 1]$ . Alternatively, the modern experimental platforms exploit the homodyne tomography to perform the detection. It uses a challenging match of a local oscillator to the output mode of a cavity with an atom [1] and can be used to estimate density matrix in Fock state basis or Wigner function in the phase space. With the knowledge of the density matrix, the quantum non-Gaussianity is given in the probabilities  $p_1 = \langle 1|\rho|1\rangle$  and  $p_{2+} = 1 - \langle 0|\rho|0\rangle - \langle 1|\rho|1\rangle$  by exceeding the threshold

$$p_1 = 2e^{\frac{t-1}{2t}} \frac{1-t}{\sqrt{t(1+t)^2}}; p_{2+} = 1 - 2e^{\frac{t-1}{2t}} \frac{1+t^2}{\sqrt{t(1+t)^2}}, \quad (3)$$

where  $t \in (0, 1]$  parametrizes the threshold again.

Using the homodyne tomography, the quantum non-Gaussianity manifests itself by the negativity of the Wigner function [22] as well. However, the negativity always vanishes for  $-3$  dB of loss, which is too challenging for many experimental platforms in optics [3]. Contrary, the criteria (3) and (3) impose no fundamental limit on the losses. Simultaneously, they are more demanding on the quality of prepared states than the nonclassical criterion [28, 29] rejecting all classical waves. In spite of that, it was demonstrated both theoretically [30] and experimentally that the criteria (3) and (3) are feasible for solid state sources [31] and atomic sources [32] when the negativity of the Wigner function disappears completely due to optical losses. The quantum non-Gaussianity of such states was recognized as a useful indicator for safety in quantum communication [33]. However, no test has been done yet for the atomic or solid-state emitters in the cavity.

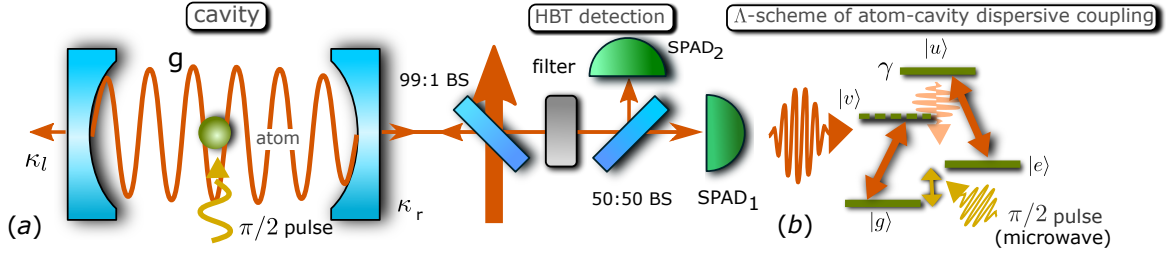


Figure 1: Quantum non-Gaussian light from a single atom in a leaky cavity. (a) A scheme for preparation and detection of quantum non-Gaussian light from a cavity. A pulsed laser beam (orange) goes through a BS with very low reflectivity and small portion of the beam is reflected towards a cavity where it interacts with an atom dispersively (see (b)). The mirrors of the cavity exhibit losses  $\kappa_l$  and  $\kappa_r$ . The state of the atom is simultaneously manipulated by a microwave field during the interaction. The light leaving the cavity is measured in the Hanbury Brown and Twiss detection set-up. It comprises a beam-splitter (BS), which divides the impinging state of light between two single-photon avalanche photo-diodes SPAD<sub>1</sub> and SPAD<sub>2</sub>. (b) A scheme of the employed energy transitions forming the  $\Lambda$ -system. The laser pulse (orange wave) entering the cavity drives the transition between states  $|e\rangle$  and  $|u\rangle$  resonantly and  $|g\rangle$  and  $|u\rangle$  off-resonantly through the virtual level  $|v\rangle$ . The state  $|u\rangle$  can decay spontaneously (light orange wave) with the rate  $\gamma$ . Initial atomic state  $(|g\rangle + |e\rangle)/\sqrt{2}$  causes entanglement between the light emerging the cavity and the atom. Simultaneous interaction of the atom with  $\pi/2$  microwave pulse (yellow wave) addressing the transition between  $|g\rangle$  and  $|e\rangle$  yields the state (7) that can exhibit heralded quantum non-Gaussian light by measuring the atomic state.

### 3 Singleatom dispersively coupled to a cavity

A prospective platform that enables diverse generation and detection of the quantum non-Gaussian light from a single atom coupled dispersively to a cavity is depicted in Fig. 1 (a). The BS with very small reflectivity splits a weak coherent state from the pumping beam and the coherent state enters the cavity mediating the interaction between light in the cavity mode and an atom. Fig. 1 (b) presents atomic relevant energy levels forming the  $\Lambda$ -scheme. Whereas the transition between states  $|e\rangle$  and  $|u\rangle$  is coupled to the cavity mode the transition between states  $|g\rangle$  and  $|u\rangle$  is strongly detuned from the cavity mode. A cavity operating in the strong coupling regime [34] induces dispersive coupling between the atom and light inside the cavity, which allows the atom to control the phase of a coherent state leaving the cavity [7]. If the atom is in the state  $|g\rangle$ , the cavity acts as a mirror due to off-resonant coupling with cavity mode and the entering coherent state is reflected with  $\pi$  phase shift in this case. When the atom occupies the state  $|e\rangle$ , the strong coupling with the cavity mode induces significant detuning of the cavity dressed states from the frequency of the incoming coherent state. Thus, the reflected state remains a coherent state, which experiences no phase shift [35, 36]. Preparing the atom initially in the superposition  $(|g\rangle + |e\rangle)/\sqrt{2}$

gives rise to entanglement between light leaving the cavity and the atomic state [1]. Employing simultaneously a microwave pulse that causes  $\pi/2$  rotation between the states  $|g\rangle$  and  $|e\rangle$  allows us to generate a state

$$|\psi\rangle = \frac{1}{\sqrt{N(\alpha)}} [(|\alpha\rangle - |-\alpha\rangle)|e\rangle + (|\alpha\rangle + |-\alpha\rangle)|g\rangle], \quad (4)$$

where  $\alpha$  is the amplitude of the coherent state entering the cavity and  $N(\alpha)$  is such that  $\langle\psi|\psi\rangle = 1$  [37]. Thus, projection to the atomic state  $|e\rangle$  heralds the state of light

$$|\psi_{-}\rangle = \frac{1}{\sqrt{2 - 2\exp(-|\alpha|^2)}}(|\alpha\rangle - |-\alpha\rangle), \quad (5)$$

where the superposition of the coherent states with different phase has the capacity to exhibit the quantum non-Gaussianity due to negative Wigner function, in principle, for any  $\alpha$ .

A realistic platform suffers from optical leakage from the cavity and dissipating emission from the atom. Simultaneously, the temporal shape of the reflected optical pulse gets distorted from the entering pulse when the amplitude  $\alpha$  becomes large [35]. Both these imperfections limit recognition of the quantum non-Gaussianity not only for atoms but also for solid state systems. Further, we consider realistic states induced by the entering optical pulse with small amplitude  $\alpha$ . Then, the pulse distortion can be neglected and the quantum non-Gaussianity gets lost mainly

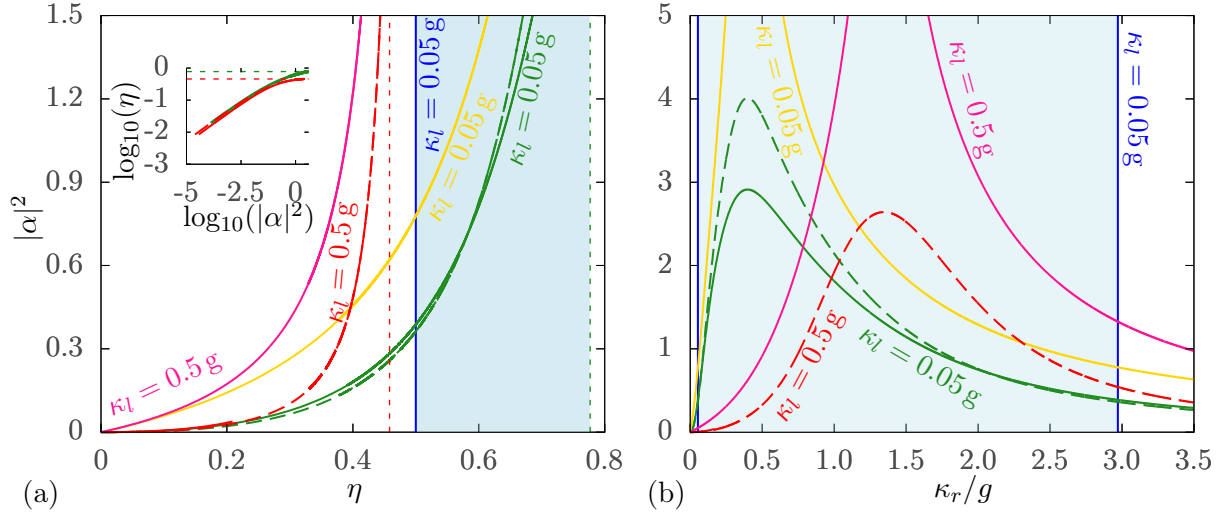


Figure 2: Quantum non-Gaussianity of light emitted by a single atom in a cavity in terms of the parameters of the dispersive interaction. The quantum non-Gaussianity manifests itself up to some threshold intensity  $|\alpha|^2$  of the incident coherent light that is depicted against the cumulative parameter  $\eta$  (a) and cavity output decay rate  $\kappa_r$  normalized to atom-cavity coupling rate  $g$  (b). In both figures, the solid and dashed lines represent the thresholds on  $|\alpha|^2$  varying with  $\kappa_r$  for fixed spontaneous emission rate  $\gamma = 0.32g$  and cavity damping rate either  $\kappa_l = 0.05g$  or  $\kappa_l = 0.5g$ . The colors differentiate values of  $\kappa_l$ . Whereas the red and green solid lines present threshold imposed by criterion (3) employing respond from SPADs, the same lines in dashed show threshold using criterion (3) for homodyne detection. The red and green dashed vertical lines in (a) represent physical boundary for the parameter  $\eta$  when  $\kappa_l = 0.5g$  and  $\kappa_l = 0.05g$  respectively. In both figures, the thresholds for cavity with damping rate  $\kappa_l = 0.05g$  (green lines) are compared with states that allow us to detect negativity in the Wigner function (the light blue region). The cavity with damping rate  $\kappa_l = 0.05g$  does not enable observation of the negativity. A condition imposed by the criterion of nonclassicality  $P_s^2 - P_e > 0$  employing SPADs [28] is given by the yellow and pink solid lines. The inset plot in (a) zooms the region of small  $|\alpha|^2$  and  $\eta$  in logarithmic scale. Briefly, (a) demonstrates that the quantum non-Gaussianity can be detected for much smaller  $\eta$  than the negativity of the Wigner function if the pumping power is low. Contrary, (b) shows that varying  $\kappa_r$  effects strongly the maximal intensity  $|\alpha|^2$  allowing the quantum non-Gaussianity to be exposed.

due to the leakage from the cavity or dissipating emission from the atom. Let  $g$  denotes the atom-cavity coupling rate between the transition  $|e\rangle\text{-}|u\rangle$  and the cavity mode. The excitation to the atomic state  $|u\rangle$  can cause a photon is spontaneously emitted with rate  $\gamma$ . Also, the mirrors effects leakage of light towards the detector and towards the environment, which happens with rates  $\kappa_r$  and  $\kappa_l$ , respectively. Considering these processes in the dynamics of the light coupled the atom allows us to establish the approximate density matrix of the heralded state emerging from the cavity [35]

$$\rho_- = \frac{1}{2(1 - e^{-2\eta|\alpha|^2})} [|\alpha_e\rangle\langle\alpha_e| + |\alpha_g\rangle\langle\alpha_g| \quad (6)$$

$$-e^{-2(1-\eta)\eta|\alpha|^2} (|\alpha_e\rangle\langle\alpha_g| + |\alpha_g\rangle\langle\alpha_e|)], \quad (7)$$

where the amplitudes of the coherent states  $|\alpha_e\rangle$

and  $|\alpha_g\rangle$  obey

$$\alpha_g = \frac{\kappa_l - \kappa_r}{\kappa_l + \kappa_r} \alpha, \quad \alpha_e = \frac{g^2 + (\kappa_l - \kappa_r)\gamma}{g^2 + (\kappa_l + \kappa_r)\gamma} \alpha. \quad (8)$$

The cumulative parameter  $\eta$  in (7)

$$\eta = \frac{\kappa_r}{\kappa_l + \kappa_r} \frac{g^2}{g^2 + \gamma(\kappa_l + \kappa_r)}. \quad (9)$$

determines the purity of the state (7). The strong-coupling regime [34] signifies  $1 - \eta \ll 1$ , for which  $\rho_-$  approaches (5) asymptotically. According to (9), the cavity has inherent imperfections quantified by  $\kappa_l$  and  $\gamma$ , which reduce  $\eta$  beyond the strong coupling regime. The parameter  $\kappa_r$  has non-trivial impacts on  $\eta$ . Very small  $\kappa_r$  causes that the emission of the light towards the SPADs is weak since the light is kept inside the cavity. Contrary, high  $\kappa_r$  increases intensity of the light impinging on the SPADs but it reduces

the parameter  $\eta$ . With fixed  $\gamma > 0$  and  $\kappa_l > 0$ , the maximal  $\eta$  occurs for [38]

$$\kappa_r = \sqrt{\frac{\kappa_l}{\gamma}} \sqrt{g^2 + \gamma \kappa_l}, \quad (10)$$

which expresses how the cavity can be engineered to maximize purity of the state  $\rho_-$ .

The state (5) exhibits Wigner function with fringes of the negative regions, which proves the quantum non-Gaussianity. However, the negativity is sensitive to the optical leakage from the cavity and dissipative emission from the atom. Thus, the state  $\rho_-$  manifests negative Wigner function only for  $\eta > 1/2$  (see Supplementary Material for details concerning derivation). Considering  $\kappa_r$  in (10), the other parameters allow us to detect the negative Wigner function only when

$$\kappa_l \gamma < \frac{g^2}{8}. \quad (11)$$

It shows that the product  $\kappa_l \gamma$  is a key parameter for exhibition of the negativity in the Wigner function. It implies that the negativity requires sufficient suppression of either  $\gamma$  or  $\kappa_l$  (ideally both) with respect to small  $g$  and  $\kappa_r$  that approaches the optimal one given by (10).

The threshold (3) employing a response from SPADs can be surpassed even when condition (11), which is necessary for the negativity of the Wigner function, fails. We evaluated manifestation of the quantum non-Gaussianity by using the criterion that the threshold (3) yields. It imposes condition on the parameter  $\eta$  that vary with the intensity  $|\alpha|^2$  of the entering coherent state. Fig. 2 presents results of this numerical analysis for two different states (7). One of the state is given by  $\gamma = 0.32g$  and  $\kappa_l = 0.05g$ , which represent the parameters of the performed experiment in [1]. These parameters fulfill the condition (11) allowing us to observe the negativity of the Wigner function for a proper choice of  $\kappa_r$ . The other state emerges the cavity with  $\kappa_l = 0.5g$  and  $\gamma = 0.32g$ . Due to (11), its Wigner function is positive for any  $\kappa_r$  and  $|\alpha|^2 > 0$ . Fig. 2 a) presents a condition the quantum non-Gaussianity imposes on the cumulative parameter  $\eta$  with respect to the intensity  $|\alpha|^2$  for the fixed parameters  $\kappa_l$  and  $\gamma$ . In both considered states, the criterion (3) reveals the quantum non-Gaussianity even for situations when the Wigner function is completely positive as the figure demonstrates. Although the parameter  $\eta$

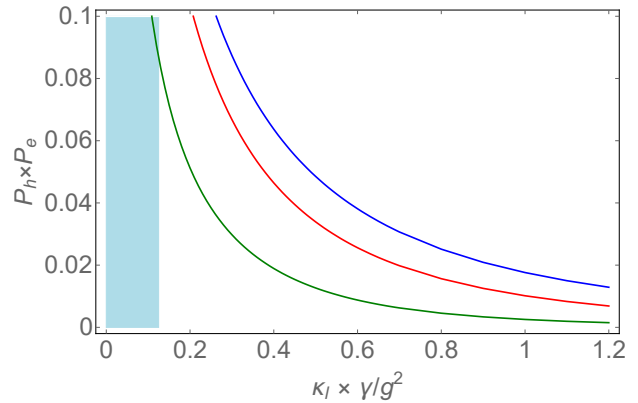


Figure 3: The maximal probability  $P_h \times P_e$  that allows recognition of the quantum non-Gaussianity against the product of parameters  $\kappa_l \times \gamma/g^2$  and  $k_r$  achieving the value  $\kappa_{r,0}$  from (10) (blue), 75% of  $\kappa_{r,0}$  (red) and 50% of  $\kappa_{r,0}$  (green) where  $\kappa_{r,0}$  maximizes  $|\alpha|^2$  that fulfills the quantum non-Gaussian criterion. Further growth of  $P_h \times P_e$  effected by increasing the intensity  $|\alpha|^2$  of the pumping beam causes the failure in the recognition. The light blue stripe depicts cases with  $\kappa_l \gamma/g^2 < 1/8$ , which enables detection of the negativity in the Wigner function when  $\kappa_r$  obeys (10).

is convenient for identifying the negativity of the Wigner function, its quantification of the cavity for the quantum non-Gaussianity is not so intelligible. Thus, the same results are presented in Fig. 2 b) in terms of  $\kappa_r$  (normalized to fixed  $g$ ) instead of  $\eta$ . It clearly demonstrates  $\kappa_r$  reaching the value in (10) determines the maximal  $|\alpha|^2$  that allows the state (7) to fulfill the criterion. The size of  $|\alpha|^2$  becomes crucial in analysis of the experimental error bars as described further. Also, both Figs. 2 a) and 2 b) present difference in the quantum non-Gaussianity manifestation employing the detection scheme with SPADs and homodyne tomography according to the criteria (3) and (3) respectively. Both requirements become almost identical for states with  $|\alpha|^2 \ll 1$ . Beyond that regime the conditions diverse themselves substantially only for the cavity obeying (11), in which case the criterion (3) employing SPADs tolerates higher  $|\alpha|^2$ . Finally, these two figures compare the conditions for the quantum non-Gaussianity with the nonclassical condition that is less demanding on  $\eta$  for a given  $|\alpha|^2$  than the quantum non-Gaussianity.

The criterion (3) imposes no fundamental limit on the parameter  $\eta$ , i. e. any  $\eta > 0$  allows us to observe the quantum non-Gaussianity if  $|\alpha|^2$  is sufficiently small. However, the intensity  $|\alpha|^2$

influences experimental time in recognition of the quantum non-Gaussianity since uncertainty in experimental estimation of the probabilities  $P_s$  and  $P_e$  depends on a number of click events, which grows with  $|\alpha|^2$ . Simultaneously,  $|\alpha|^2$  affects the probability  $P_h$  of successful heralding the state  $\rho_-$ , which is given by projection to the atomic state  $|e\rangle$ , according to  $P_h = 1 - e^{-2\eta|\alpha|^2}$ . It suggests the appropriate intensity  $|\alpha|^2$  is given by the trade-off between the overall measurement time and requirement imposed by the suppression of the threshold (3). Fig. 3 presents the rate  $P_h \times P_e$  for states achieved from the maximal intensity  $|\alpha|^2$  of the pumping beam that the quantum non-Gaussianity tolerates. Note, the rate is always lower in real detection of the quantum non-Gaussianity since it has to be arranged by  $|\alpha|^2$  such that the measured probabilities  $P_s$  and  $P_e$  surpass the threshold even within their error bars.

## 4 Realistic cavity with noise contributions

Realistic systems can be further affected by small noise contributions from emitter, stray light or measurement dark counts. We test our prediction under noise impacts by considering multiphoton effects of the displacement operator  $D(\nu) = \exp(\nu a^\dagger - \nu^* a)$  with the random amplitude  $\nu$  on the emerging light. Thus, the density matrix deteriorated by the noise obtains

$$\rho = \int d^2\nu P(\nu) D(\nu) \rho_- D^\dagger(\nu) \quad (12)$$

with  $P(\nu)$  being a density probability function identifying the stochastic processes affecting the amplitude  $\nu$ . We can analyse two typically relevant stochastic processes. In the first case only the phase of  $\nu$  undergoes the fluctuation, i. e.  $P_P(\nu) = \delta(|\nu|^2 - \bar{n}) / (2\pi)$ . In the second case, we allow for  $P_{BE}(\nu) = \exp\{-[(\nu + \nu^*)^2 + (\nu - \nu^*)^2] / (4\bar{n})\} / (\pi\bar{n})$ , and therefore the amplitude  $\nu$  changes randomly both the phase and its size. The model of the noise in (12) with the probability distribution function  $P_P(\nu)$  corresponds to the Poissonian noise and the model induced by the probability distribution function  $P_{BE}(\nu)$  describes the Bose-Einstein noise. Supplementary Material presents how the Poissonian noise and the Bose-Einstein noise in-

fluence the manifestation of the quantum non-Gaussianity for specific values of  $\bar{n}$ . In the region of very weak pumping power  $|\alpha|^2 \ll 1$  and small mean number of noisy photons  $\bar{n} \ll 1$ , the probabilities obey the approximation

$$P_s \approx \frac{\eta}{2} \quad (13)$$

$$P_e \approx \frac{\eta [(\eta - 1)g^2 + 2\eta\gamma\kappa]^2}{g^4} |\alpha|^2 + \eta\bar{n} \quad (14)$$

for both the Poissonian noise and the thermal noise. Since the criterion becomes approximated by  $P_s^3 > P_e/4$  for the surpassed probability  $P_e$ , the quantum non-Gaussianity imposes an approximate condition

$$|\alpha|^2 + \bar{n} < \frac{\eta^2}{2}, \quad (15)$$

which expresses the limitation on  $|\alpha|^2$  involving the impacts of the noise. If  $\bar{n} \geq \eta^2/2$  the quantum non-Gaussianity is recognized for no  $|\alpha|^2$ . Let us remind that (12) introduces model of narrow-band noise, which contributes to the mode occupied by the light from cavity. A model of broad-band (incoherent) Poissonian noise, which contributes independently to many modes, gives rise to the less demanding approximate condition  $2|\alpha|^2 + \bar{n} < \eta^2$  with  $\bar{n}$  being the mean number of noisy photons.

## 5 Conclusion and Outlook

To conclude, we proved that light emitted from an dispersively coupled atom or solid state emitter inside a cavity manifests the quantum non-Gaussianity much broadly under realistic conditions of current experiments. The only limitation for the recognition can be a background noise deteriorating the measured light. High intensity of the pumping coherent beam, which prevents the recognition as well, can be always reduced with the cost of decreasing the overall rates. Simultaneously, this detection can be employed to expose the quantum non-Gaussianity of light from a quantum dot inside a micropillar cavity [39] or a photonics crystal [8]. A possible modification of the criterion can be applied for exposing the quantum non-Gaussianity of the cat states and, further, the Gottesman-Kitaev-Preskill states [40]. After the experimental tests, quantum non-Gaussian depth can be investigated

to compare quality of emitted states. Using more atoms in the cavity, future higher Fock state preparation can be evaluated using the existing hierarchy of quantum non-Gaussianity [41].

## Acknowledgments

R. F. and L. L. acknowledge project 21-13265X of the Czech Science Foundation. J. K. V. acknowledges the MSMT of the Czech Republic and Horizon 2020 Framework Programme (731473, project 8C20002 ShoQC).

## A Appendix: A single atom dispersively coupled to a cavity

Let an pulsed laser light enters a cavity where an atom with energy levels forming the  $\Lambda$ -system is coupled to the cavity mode. Under assumptions mentioned in [35], the heralded light leaving the cavity approaches the density matrix [1]

$$\rho_- = \frac{1}{2(1 - e^{-2\eta|\alpha|^2})} [|\alpha_e\rangle\langle\alpha_e| + |\alpha_g\rangle\langle\alpha_g| - e^{-2(1-\eta)\eta|\alpha|^2} (|\alpha_e\rangle\langle\alpha_g| + |\alpha_g\rangle\langle\alpha_e|)], \quad (16)$$

where  $|\alpha_e\rangle$  and  $|\alpha_g\rangle$  are coherent states with the amplitudes

$$\alpha_g = \frac{\kappa_l - \kappa_r}{\kappa_l + \kappa_r} \alpha, \quad \alpha_e = \frac{g^2 + (\kappa_l - \kappa_r)\gamma}{g^2 + (\kappa_l + \kappa_r)\gamma} \alpha. \quad (17)$$

with  $\alpha$  being the amplitude of the incoming coherent state. The parameter  $\eta$  in (16) is defined by the identity

$$\eta|\alpha| = \frac{1}{2}|\alpha_e - \alpha_g|, \quad (18)$$

which gives rise to

$$\eta = \frac{\kappa_r}{\kappa_l + \kappa_r} \frac{g^2}{g^2 + \gamma(\kappa_l + \kappa_r)}. \quad (19)$$

It shows how the cavity parameters reduces the difference (18). A cavity operating in the strong coupling regime when  $g \gg \gamma$  and  $g \gg \kappa_r \gg \kappa_l$  allows us to approach  $\eta = 1$ . Beyond that regime, the cumulative parameter  $\eta$  is always reduced below one, which affects the purity of the state  $\rho_-$ .

### A.1 Wigner function

The Wigner function  $W(\alpha, \alpha^*)$  enables recognition of the quantum non-Gaussianity when it exhibits negativity. To determine its value for the states  $\rho_-$ , we consider the relation

$$W(\beta, \beta^*) = \frac{1}{2\pi} \langle D^\dagger(\beta) (-1)^{a^\dagger a} D(\beta) \rangle, \quad (20)$$

where  $a^\dagger$  and  $a$  are creation and annihilation operator and  $D(\beta) = \exp(\beta a^\dagger - \beta^* a)$  is the displacement operator [42]. Let us introduce the state

$$\tilde{\rho}_- = D[-(\alpha_e + \alpha_g)/2] \rho_- D^\dagger[-(\alpha_e + \alpha_g)/2]. \quad (21)$$

The displacement operator in (21) shifts the state  $\rho_-$  such that the negative region (if there is any) is in the origin. Thus, employing the identities (7) and (17) yields

$$\begin{aligned} \tilde{\rho}_- = & \\ & \frac{1}{2(1 - e^{-2\eta|\alpha|^2})} [|\eta\alpha\rangle\langle\eta\alpha| + |-\eta\alpha\rangle\langle\eta\alpha| \\ & - e^{-2(1-\eta)\eta|\alpha|^2} (|\eta\alpha\rangle\langle-\eta\alpha| + |-\eta\alpha\rangle\langle\eta\alpha|)] \end{aligned} \quad (22)$$

The state  $\tilde{\rho}_-$  is formally identical to the state  $|\psi\rangle \propto (|\alpha\rangle - |-\alpha\rangle)$  that undergoes losses quantified by the transmission  $\eta$ . Due to that, the negativity remains only for  $\eta > 1/2$  [25].

## B Appendix: Effects of the noise

The density matrix (7) represents an emitted light, which is not affected by noise. To include the noise contributions in the description, we allow for a scenario when the light is influenced by acting the displacement operator with a fluctuating amplitude. Thus, the noise affects the density matrix according to

$$\rho = \int d^2\beta P(\beta) D(\beta) \rho_- D^\dagger(\beta), \quad (23)$$

where  $D(\beta) = \exp(\beta a^\dagger - \beta^* a)$  is the displacement operator. The amplitude  $\beta$  undergoes random fluctuations that the density probability function  $P(\beta)$  determines. Further, we assume two fundamental stochastic processes for which the density probability functions yield

$$\begin{aligned} P_P(\beta) &= \frac{1}{2\pi} \delta(|\beta| - \sqrt{\bar{n}}) \\ P_{BE}(\beta) &= \frac{1}{\pi\bar{n}} e^{-\frac{|\beta|^2}{\bar{n}}}, \end{aligned} \quad (24)$$

where  $\bar{n}$  is mean number of the noisy photons. When  $P_P(\beta)$  is taken into account, the amplitude  $\beta$  experiences random fluctuation in phase only. Contrary,  $P_{BE}(\beta)$  represents fluctuation in both the phase and the intensity  $|\beta|^2$ . Let us call the noise identified by the density probability functions  $P_P(\beta)$  Poissonian noise and the noise given by  $P_{BE}(\beta)$  Bose-Einstein noise according to distribution of noisy photons that are produce when the stochastic displacement affects the vacuum states.

To obtain formulas for the click probabilities, let us deal with the state  $\rho_{-, \beta} = D(\beta) \rho_- D^\dagger(\beta)$

before considering the stochastic processes. Its density matrix works out to

$$\begin{aligned} \rho_{-, \beta} = & \frac{1}{2(1 - e^{-2\eta|\alpha|^2})} \{ |\bar{\alpha}_{e, \beta}\rangle\langle\bar{\alpha}_{e, \beta}| + |\bar{\alpha}_{g, \beta}\rangle\langle\bar{\alpha}_{g, \beta}| \\ & - e^{-2(1-\eta)\eta|\alpha|^2} \times [ e^{\eta(\beta\alpha^* - \beta^*\alpha)} |\bar{\alpha}_{e, \beta}\rangle\langle\bar{\alpha}_{g, \beta}| \\ & + e^{\eta(\beta^*\alpha - \beta\alpha^*)} |\bar{\alpha}_{g, \beta}\rangle\langle\bar{\alpha}_{e, \beta}| ] \}, \end{aligned} \quad (25)$$

where  $\bar{\alpha}_{e, \beta} = \alpha_e + \beta$  and  $\bar{\alpha}_{g, \beta} = \alpha_g + \beta$ . Let the state  $\rho_{-, \beta}$  go through a balanced BS. Outgoing state  $\bar{\rho}_{-, \beta}$  in the transmitted mode is given by

$$\begin{aligned} \bar{\rho}_{-, \beta} = & \\ & \frac{1}{2(1 - e^{-2\eta|\alpha|^2})} \{ |\bar{\alpha}_{e, \beta}/\sqrt{2}\rangle\langle\bar{\alpha}_{e, \beta}/\sqrt{2}| \\ & + |\bar{\alpha}_{g, \beta}/\sqrt{2}\rangle\langle\bar{\alpha}_{g, \beta}/\sqrt{2}| \\ & - e^{-2(1-\eta)\eta|\alpha|^2 - \eta^2|\alpha|^2 + [\beta^*(\alpha_g + \alpha_e) + \beta(\alpha_g^* + \alpha_e^*)]/4} \\ & \times [ e^{(\alpha_e^*\beta + \alpha_g\beta^*)/2 + \eta(\beta\alpha^* - \beta^*\alpha)} |\bar{\alpha}_{e, \beta}/\sqrt{2}\rangle\langle\bar{\alpha}_{g, \beta}/\sqrt{2}| \\ & + e^{(\alpha_e\beta^* + \alpha_g^*\beta)/2 + \eta(\beta^*\alpha - \beta\alpha^*)} \\ & \times |\bar{\alpha}_{g, \beta}/\sqrt{2}\rangle\langle\bar{\alpha}_{e, \beta}/\sqrt{2}| ] \}. \end{aligned} \quad (27)$$

The density matrix of the incident state (25) and transmitted state (27) allows us to determine how  $\beta$  influences the click probability  $P_s(\beta) = 1 - \langle 0 | \bar{\rho}_{-, \beta} | 0 \rangle$  and double click  $P_e(\beta) = 1 - 2\langle 0 | \bar{\rho}_{-, \beta} | 0 \rangle + \langle 0 | \rho_{-, \beta} | 0 \rangle$ . Thus, the click probability  $P_s$  and double click probability  $P_c$  of the noisy state (23) read

$$\begin{aligned} P_s &= \int d^2\beta P(\beta) P_s(\beta) \\ P_e &= \int d^2\beta P(\beta) P_e(\beta) \end{aligned} \quad (28)$$

with  $P(\beta)$  being some density probability function from (24). We provide only the approximate formulas for  $P_s$  and  $P_e$  appropriate for states with  $|\alpha|^2 \ll 1$  and  $\bar{n} \ll 1$ . Under these assumptions, they get simplified to

$$P_s = \frac{\eta}{2} \quad (29)$$

$$P_c = \frac{\eta [(\eta - 1)g^2 + 2\eta\gamma\kappa]^2}{g^4} |\alpha|^2 + \eta\bar{n}, \quad (30)$$

for both the noise, which are considered. Fig. 4 depicts when the noise contribution enable recognition of the quantum non-Gaussianity for some specific settings of the cavity parameters.

The model of noisy states (23) can be modified to a model in which the noise contributes as independent background noise, i. e. the density matrix reads  $\rho = \rho_- \otimes \rho_{\bar{n}}$ , where  $\rho_{\bar{n}}$  obeys



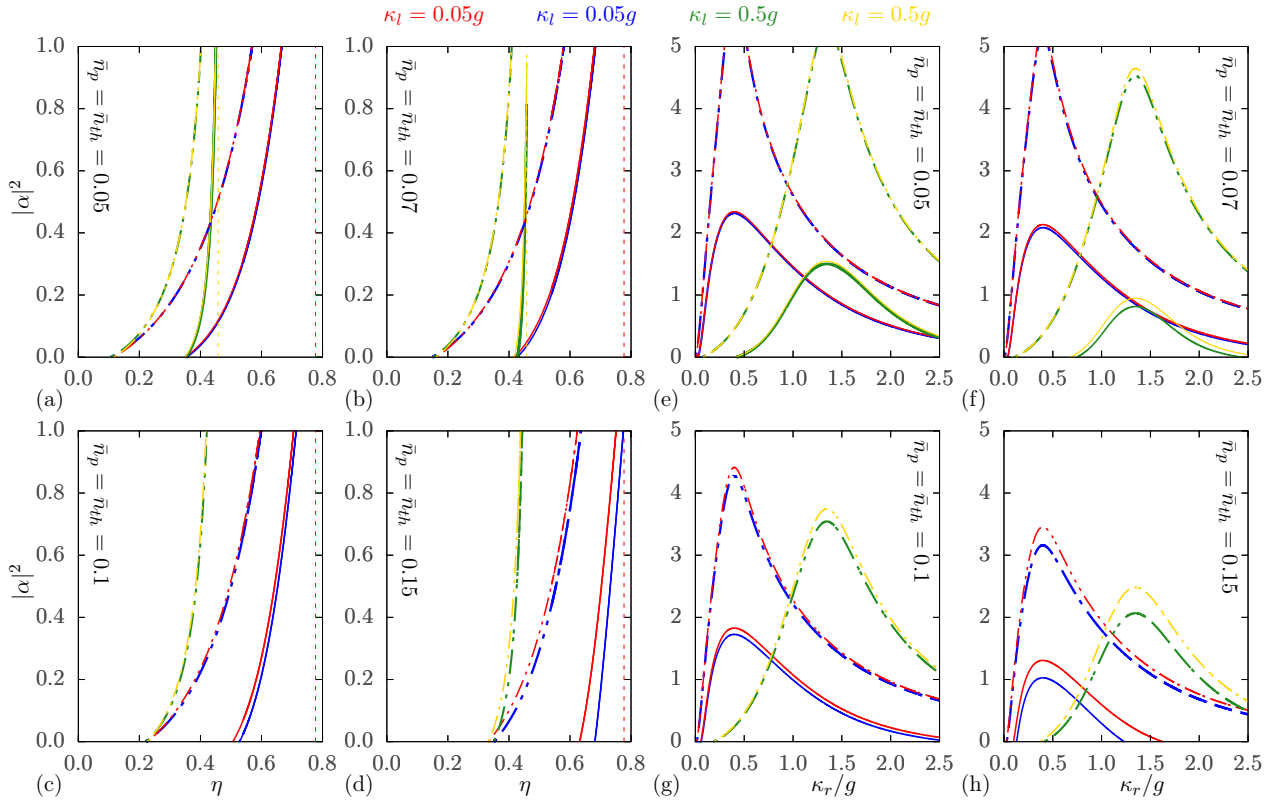


Figure 4: Thresholds for exposing the quantum non-Gaussianity of noisy states (23) in terms of pumping intensity  $|\alpha|^2$  and either cumulative parameter  $\eta$  (a)-(d) or the parameter  $\kappa_r$  normalized to  $g$  (e)-(h). Each sub-figure allows for different mean number of noisy photons  $\bar{n}$ . Whereas the blue and green solid lines represent the Poissonian noise deteriorating the light, the red and golden solid lines correspond to the Bose-Einstein noise. Also, the colors differentiate the parameter  $\kappa_r$  as labeled by respective color above each plot. The spontaneous emission rate  $\gamma$  is set to  $\gamma = 0.32g$  for each sub-figure. Finally, each line of given color is plotted as solid and dashed, which distinguish the threshold derived for detection employing the SPADs (solid) and PNRDs (dashed). The quantum non-Gaussianity manifests itself for states with  $\eta$  above the respective line in sub-figures (a)-(d). The horizontal red and yellow dashed lines represent there the physical boundary for  $\eta$  when  $\kappa_l = 0.05g$  and  $\kappa_l = 0.5g$  respectively. The quantum non-Gaussianity is certified for  $|\alpha|^2$  below the respective lines.

the Poissonian distribution of photons with mean number of photons  $\bar{n}$ . In this case, the click probabilities in the limit of  $|\alpha|^2 \ll 1$  and  $\bar{n} \ll 1$  works out to be

$$P_s = \frac{\eta}{2} \quad (31)$$

$$P_c = \frac{\eta [(\eta - 1)g^2 + 2\eta\gamma\kappa]^2}{g^4} |\alpha|^2 + \frac{\eta\bar{n}}{2}. \quad (32)$$

Comparing (30) with (32) suggests that the background noise has less impacts on the probability  $P_c$ . Consequently, the quantum non-Gaussianity is more sensitive to contributions of noise in (23) than to the contributions of the background noise.

## References

- [1] Bastian Hacker, Stephan Welte, Severin Daiss, Armin Shaukat, Stephan Ritter, Lin Li, and Gerhard Rempe. Deterministic creation of entangled atom–light schrödinger-cat states. *Nature Photonics*, 13(2):110–115, 2019. DOI: [10.1038/s41566-018-0339-5](https://doi.org/10.1038/s41566-018-0339-5).
- [2] Jeremy L. O'Brien, Akira Furusawa, and Jelena Vučković. Photonic quantum technologies. *Nature Photonics*, 3(12):687–695, 2009. DOI: [10.1038/nphoton.2009.229](https://doi.org/10.1038/nphoton.2009.229).
- [3] Igor Aharonovich, Dirk Englund, and Milos Toth. Solid-state single-photon emitters. *Nature Photonics*, 10(10):631–641, 2016. DOI: [10.1038/nphoton.2016.186](https://doi.org/10.1038/nphoton.2016.186).
- [4] Xu-Jie Wang, Sheng-Jun Yang, Peng-Fei Sun, Bo Jing, Jun Li, Ming-Ti Zhou, Xiao-

- Hui Bao, and Jian-Wei Pan. Cavity-enhanced atom-photon entanglement with subsecond lifetime. *Physical Review Letters*, 126(9):090501, 2021. DOI: [10.1103/physrevlett.126.090501](https://doi.org/10.1103/physrevlett.126.090501).
- [5] Fabian Wolf, Chunyan Shi, Jan C. Heip, Manuel Gessner, Luca Pezzè, Augusto Smerzi, Marius Schulte, Klemens Hammerer, and Piet O. Schmidt. Motional fock states for quantum-enhanced amplitude and phase measurements with trapped ions. *Nature Communications*, 10(1), 2019. DOI: [10.1038/s41467-019-10576-4](https://doi.org/10.1038/s41467-019-10576-4).
- [6] Alán Aspuru-Guzik and Philip Walther. Photonic quantum simulators. *Nature Physics*, 8(4):285–291, 2012. DOI: [10.1038/nphys2253](https://doi.org/10.1038/nphys2253).
- [7] L.-M. Duan and H. J. Kimble. Scalable photonic quantum computation through cavity-assisted interactions. *Physical Review Letters*, 92(12):127902, 2004. DOI: [10.1103/physrevlett.92.127902](https://doi.org/10.1103/physrevlett.92.127902).
- [8] Peter Lodahl, Sahand Mahmoodian, and Søren Stobbe. Interfacing single photons and single quantum dots with photonic nanostructures. *Reviews of Modern Physics*, 87(2):347–400, 2015. DOI: [10.1103/revmodphys.87.347](https://doi.org/10.1103/revmodphys.87.347).
- [9] M. Arcari, I. Söllner, A. Javadi, S. Lindskov Hansen, S. Mahmoodian, J. Liu, H. Thyrrerstrup, E.H. Lee, J.D. Song, S. Stobbe, and P. Lodahl. Near-unity coupling efficiency of a quantum emitter to a photonic crystal waveguide. *Physical Review Letters*, 113(9):093603, 2014. DOI: [10.1103/physrevlett.113.093603](https://doi.org/10.1103/physrevlett.113.093603).
- [10] N. Somaschi, V. Giesz, L. De Santis, J. C. Loredó, M. P. Almeida, G. Hornecker, S. L. Portalupi, T. Grange, C. Antón, J. Demory, C. Gómez, I. Sagnes, N. D. Lanzillotti-Kimura, A. Lemaître, A. Auffèves, A. G. White, L. Lanco, and P. Senellart. Near-optimal single-photon sources in the solid state. *Nature Photonics*, 10(5):340–345, 2016. DOI: [10.1038/nphoton.2016.23](https://doi.org/10.1038/nphoton.2016.23).
- [11] O. Morin, M. Körber, S. Langenfeld, and G. Rempe. Deterministic shaping and reshaping of single-photon temporal wave functions. *Physical Review Letters*, 123(13):133602, 2019. DOI: [10.1103/physrevlett.123.133602](https://doi.org/10.1103/physrevlett.123.133602).
- [12] Petr Zapletal and Radim Filip. Multi-copy quantifiers for single-photon states. *Scientific Reports*, 7(1), 2017. DOI: [10.1038/s41598-017-01333-y](https://doi.org/10.1038/s41598-017-01333-y).
- [13] Joonsuk Huh, Gian Giacomo Guerreschi, Borja Peropadre, Jarrod R. McClean, and Alán Aspuru-Guzik. Boson sampling for molecular vibronic spectra. *Nature Photonics*, 9(9):615–620, 2015. DOI: [10.1038/nphoton.2015.153](https://doi.org/10.1038/nphoton.2015.153).
- [14] Peter Lodahl, A. Floris van Driel, Ivan S. Nikolaev, Arie Irman, Karin Overgaag, Daniël Vanmaekelbergh, and Willem L. Vos. Controlling the dynamics of spontaneous emission from quantum dots by photonic crystals. *Nature*, 430(7000):654–657, 2004. DOI: [10.1038/nature02772](https://doi.org/10.1038/nature02772).
- [15] E. Peter, P. Senellart, D. Martrou, A. Lemaître, J. Hours, J. M. Gérard, and J. Bloch. Exciton-photon strong-coupling regime for a single quantum dot embedded in a microcavity. *Physical Review Letters*, 95(6):067401, 2005. DOI: [10.1103/physrevlett.95.067401](https://doi.org/10.1103/physrevlett.95.067401).
- [16] Xiao-Liu Chu, Stephan Götzinger, and Vahid Sandoghdar. A single molecule as a high-fidelity photon gun for producing intensity-squeezed light. *Nature Photonics*, 11(1):58–62, 2016. DOI: [10.1038/nphoton.2016.236](https://doi.org/10.1038/nphoton.2016.236).
- [17] Xing Ding, Yu He, Z.-C. Duan, Niels Gregersen, M.-C. Chen, S. Unsleber, S. Maier, Christian Schneider, Martin Kamp, Sven Höfling, Chao-Yang Lu, and Jian-Wei Pan. On-demand single photons with high extraction efficiency and near-unity indistinguishability from a resonantly driven quantum dot in a micropillar. *Physical Review Letters*, 116(2):020401, 2016. DOI: [10.1103/physrevlett.116.020401](https://doi.org/10.1103/physrevlett.116.020401).
- [18] Maximilian Prilmüller, Tobias Huber, Markus Müller, Peter Michler, Gregor Weihs, and Ana Predojević. Hyperentanglement of photons emitted by a quantum dot. *Physical Review Letters*, 121(11):110503, 2018. DOI: [10.1103/physrevlett.121.110503](https://doi.org/10.1103/physrevlett.121.110503).
- [19] Laia Ginés, Carlo Pepe, Junior Gonzales, Niels Gregersen, Sven Höfling, Christian Schneider, and Ana Predojević. Time-bin entangled photon pairs from quantum dots embedded in a self-aligned cav-

- ity. *Optics Express*, 29(3):4174, 2021. DOI: [10.1364/oe.411021](https://doi.org/10.1364/oe.411021).
- [20] C. Flühmann, T. L. Nguyen, M. Marinelli, V. Negnevitsky, K. Mehta, and J. P. Home. Encoding a qubit in a trapped-ion mechanical oscillator. *Nature*, 566(7745):513–517, 2019. DOI: [10.1038/s41586-019-0960-6](https://doi.org/10.1038/s41586-019-0960-6).
- [21] Kentaro Wakui, Hiroki Takahashi, Akira Furusawa, and Masahide Sasaki. Photon subtracted squeezed states generated with periodically poled KTiOPO<sub>4</sub>. *Optics Express*, 15(6):3568, 2007. DOI: [10.1364/oe.15.003568](https://doi.org/10.1364/oe.15.003568).
- [22] A. I. Lvovsky and M. G. Raymer. Continuous-variable optical quantum-state tomography. *Reviews of Modern Physics*, 81(1):299–332, 2009. DOI: [10.1103/revmodphys.81.299](https://doi.org/10.1103/revmodphys.81.299).
- [23] Ulrik L. Andersen, Jonas S. Neergaard-Nielsen, Peter van Loock, and Akira Furusawa. Hybrid discrete- and continuous-variable quantum information. *Nature Physics*, 11(9):713–719, 2015. DOI: [10.1038/nphys3410](https://doi.org/10.1038/nphys3410).
- [24] Daniel Huber, Marcus Reindl, Yongheng Huo, Huiying Huang, Johannes S. Wildmann, Oliver G. Schmidt, Armando Rastelli, and Rinaldo Trotta. Highly indistinguishable and strongly entangled photons from symmetric GaAs quantum dots. *Nature Communications*, 8(1), 2017. DOI: [10.1038/ncomms15506](https://doi.org/10.1038/ncomms15506).
- [25] R.L. Hudson. When is the wigner quasi-probability density non-negative? *Reports on Mathematical Physics*, 6(2):249–252, 1974. DOI: [10.1016/0034-4877\(74\)90007-x](https://doi.org/10.1016/0034-4877(74)90007-x).
- [26] R. Hanbury Brown and R.Q. Twiss. LXXIV. a new type of interferometer for use in radio astronomy. *The London, Edinburgh, and Dublin Philosophical Magazine and Journal of Science*, 45(366):663–682, 1954. DOI: [10.1080/14786440708520475](https://doi.org/10.1080/14786440708520475).
- [27] Radim Filip and Ladislav Mišta. Detecting quantum states with a positive wigner function beyond mixtures of gaussian states. *Physical Review Letters*, 106(20):200401, 2011. DOI: [10.1103/physrevlett.106.200401](https://doi.org/10.1103/physrevlett.106.200401).
- [28] Lukáš Lachman and Radim Filip. Robustness of quantum nonclassicality and non-gaussianity of single-photon states in attenuating channels. *Physical Review A*, 88(6):063841, 2013. DOI: [10.1103/physreva.88.063841](https://doi.org/10.1103/physreva.88.063841).
- [29] P Grangier, G Roger, and A Aspect. Experimental evidence for a photon anticorrelation effect on a beam splitter: A new light on single-photon interferences. *Europhysics Letters (EPL)*, 1(4):173–179, 1986. DOI: [10.1209/0295-5075/1/4/004](https://doi.org/10.1209/0295-5075/1/4/004).
- [30] Lukáš Lachman and Radim Filip. Quantum non-gaussianity from a large ensemble of single photon emitters. *Optics Express*, 24(24):27352, 2016. DOI: [10.1364/oe.24.027352](https://doi.org/10.1364/oe.24.027352).
- [31] Ivo Straka, Ana Predojević, Tobias Huber, Lukáš Lachman, Lorenz Butschek, Martina Miková, Michal Mičuda, Glenn S. Solomon, Gregor Weihs, Miroslav Ježek, and Radim Filip. Quantum non-gaussian depth of single-photon states. *Physical Review Letters*, 113(22):223603, 2014. DOI: [10.1103/physrevlett.113.223603](https://doi.org/10.1103/physrevlett.113.223603).
- [32] D B Higginbottom, L Slodička, G Araneda, L Lachman, R Filip, M Hennrich, and R Blatt. Pure single photons from a trapped atom source. *New Journal of Physics*, 18(9):093038, 2016. DOI: [10.1088/1367-2630/18/9/093038](https://doi.org/10.1088/1367-2630/18/9/093038).
- [33] Mikołaj Lasota, Radim Filip, and Vladyslav C. Usenko. Sufficiency of quantum non-gaussianity for discrete-variable quantum key distribution over noisy channels. *Physical Review A*, 96(1):012301, 2017. DOI: [10.1103/physreva.96.012301](https://doi.org/10.1103/physreva.96.012301).
- [34] Andreas Reiserer and Gerhard Rempe. Cavity-based quantum networks with single atoms and optical photons. *Reviews of Modern Physics*, 87(4):1379–1418, 2015. DOI: [10.1103/revmodphys.87.1379](https://doi.org/10.1103/revmodphys.87.1379).
- [35] B. Wang and L.-M. Duan. Engineering superpositions of coherent states in coherent optical pulses through cavity-assisted interaction. *Physical Review A*, 72(2):022320, 2005. DOI: [10.1103/physreva.72.022320](https://doi.org/10.1103/physreva.72.022320).
- [36] Hayato Goto and Kouichi Ichimura. Quantum trajectory simulation of controlled phase-flip gates using the vacuum rabi splitting. *Physical Review A*, 72(5):054301, 2005. DOI: [10.1103/physreva.72.054301](https://doi.org/10.1103/physreva.72.054301).
- [37] Severin Daiss, Stephan Welte, Bastian Hacker, Lin Li, and Gerhard Rempe. Single-photon distillation via a photonic parity measurement using cavity QED. *Physical*

- Review Letters*, 122(13):133603, 2019. DOI: [10.1103/physrevlett.122.133603](https://doi.org/10.1103/physrevlett.122.133603).
- [38] Hayato Goto, Shota Mizukami, Yuuki Tokunaga, and Takao Aoki. Figure of merit for single-photon generation based on cavity quantum electrodynamics. *Physical Review A*, 99(5):053843, 2019. DOI: [10.1103/physreva.99.053843](https://doi.org/10.1103/physreva.99.053843).
- [39] Daniel Najer, Immo Söllner, Pavel Sekatski, Vincent Dolique, Matthias C. Löbl, Daniel Riedel, Rüdiger Schott, Sebastian Starosielec, Sascha R. Valentin, Andreas D. Wieck, Nicolas Sangouard, Arne Ludwig, and Richard J. Warburton. A gated quantum dot strongly coupled to an optical microcavity. *Nature*, 575(7784):622–627, 2019. DOI: [10.1038/s41586-019-1709-y](https://doi.org/10.1038/s41586-019-1709-y).
- [40] J. Hastrup, U. L. Andersen, arXiv:2104.07981.
- [41] Lukáš Lachman, Ivo Straka, Josef Hloušek, Miroslav Ježek, and Radim Filip. Faithful hierarchy of genuine  $n$ -photon quantum non-gaussian light. *Physical Review Letters*, 123(4), 2019. DOI: [10.1103/physrevlett.123.043601](https://doi.org/10.1103/physrevlett.123.043601).
- [42] Antoine Royer. Wigner function as the expectation value of a parity operator. *Physical Review A*, 15(2):449–450, feb 1977. DOI: [10.1103/physreva.15.449](https://doi.org/10.1103/physreva.15.449).